

Non-Aqueous Thermolytic Route to Oxynitride Photomaterials using Molecular Precursors $\text{Ti(O}'\text{Bu)}_4$ and $\text{N}\equiv\text{Mo(O}'\text{Bu)}_3$

Daniel A. Ruddy,^{*a} Obadiah G. Reid,^a Brian M. Leonard,^b Svitlana Pylypenko,^c and Nathan R. Neale^{*a}

^aChemical and Materials Science Center, National Renewable Energy Laboratory, Golden, CO

^bDepartment of Chemistry, University of Wyoming, Laramie, WY

^cDepartment of Metallurgical & Materials Engineering, Colorado School of Mines, Golden, CO

Experimental

General. All manipulations were conducted under nitrogen atmosphere using standard Schlenk techniques, or under a helium atmosphere in a Vacuum Atmospheres glovebox unless otherwise noted. Dry, oxygen free solvents were used throughout the syntheses. Hexanes and toluene solvents used in the air-sensitive syntheses were dried by passing through an alumina column and were stored under nitrogen. Tetrahydrofuran and diethyl ether solvents were dried and distilled from potassium ketyl and stored under nitrogen. Benzene-*d*₆ used for NMR spectroscopy was dried and distilled from potassium ketyl and stored in the glovebox. $\text{NMo(O}'\text{Bu)}_3$ (**1**) and $\text{MoO}_2(\text{O}'\text{Bu})_2$ (**3**) were prepared according to literature procedures.^{1,2} Titanium tetrakis(*tert*-butoxide), $\text{Ti(O}'\text{Bu)}_4$, (**2**) was purchased from Sigma-Aldrich, stored in the glovebox, and used without further purification.

Preparation of $\text{Ti}_x\text{Mo(ON)}$ and Ti_xMoO materials. In a glovebox, **1** or **3** was combined with the corresponding amount of **2** to give the desired Ti/Mo mol ratio and a total of 1.5 mmol of precursors. The reagents were combined in a 23 mL Teflon sleeve with 8.0 mL of dry toluene, and sealed in a steel autoclave under helium. Complex **1** demonstrates limited solubility in toluene (and benzene-*d*₆ for NMR studies) at room temperature, however, it completely dissolves at 50 °C without any observed decomposition. The solution was pre-heated for 30 min at 100 °C to complete the dissolution, and then heated at 10 °C/min to 200 °C and

held for 6 h. After cooling to room temperature, the resulting material was transferred to a 50 mL centrifuge tube, isolated by centrifugation, and dried under flowing nitrogen for 4–6 h at room temperature. Typical yield was 120–150 mg. Alternatively, the materials can be dried under vacuum to remove residual toluene, or isolated by allowing the as-prepared material to air-dry in the Teflon sleeve in a fumehood for 5–7 days. These methods produced materials that were indistinguishable by our characterization methods.

Characterization. Solution ^1H NMR spectra were recorded using a Varian Inova 400 MHz spectrometer. Elemental analyses were performed at Galbraith Laboratories, Inc. (Knoxville, TN) and Huffman Laboratories (Golden, CO) by means of inductively-coupled plasma optical emission spectroscopy (ICP-OES) for Ti and Mo, and by combustion analysis for C, H, and N. Powder X-ray diffraction data were collected using a Rigaku Ultima IV diffractometer with a Cu $\text{K}\alpha$ source. Diffractograms were collected in the 2θ range of 20 – 80 degrees at a scan rate of 2 °/min. Samples (10–20 mg) were supported on a glass sample holder with a 0.2 mm recessed sample area and were pressed into the recession with a glass slide to obtain a uniform z-axis height. Nitrogen physisorption data were collected at 77 K using a Quantachrome Quadrasorb SI instrument. Samples (ca. 50 mg) were pre-treated under vacuum for 1 h at 25 °C to minimize loss of N from the material. Surface areas were determined using the Brunauer-Emmett-Teller (BET) method, and pore volumes and pore diameters were determined from the adsorption isotherm data using the Barrett-Joyner-Halenda (BJH) method. Samples for diffuse reflectance UV-visible-NIR (DRUV-vis-NIR) absorbance spectroscopy were prepared by pressing the powder on an Al sample holder with a 0.5 mm recessed sample area and covered with a quartz slide. Spectra were recorded using a Shimadzu UV-3600 spectrophotometer fitted with a diffuse-reflectance attachment. BaSO_4 was used as a reference. Spectra were recorded in

reflectance mode and transformed into the normalized Kubelka-Munk function using the equation, $F(R) = (I-R)^2/2R$. Thermogravimetric infrared (TG-IR) analysis was performed using ca. 10 mg of powder sample placed in a TA Instruments Q500 TGA outfitted with a quartz-lined evolved gas analysis (EGA) furnace. A Thermo Nicolet 6700 FT-IR spectrometer was coupled to the TGA with a TGA/FTIR interface consisting of a heated quartz gas cell and a heated quartz lined transfer line. The TGA furnace temperature was ramped from 30–600 °C at 10 °C/min in a flow of clean air. The transfer line was set to 225 °C and the gas cell to 250 °C with IR spectra taken at 2 cm⁻¹ resolution. TG-IR experiments determine real time mass change, evolved gas monitoring and component identification. Identification of the evolved gases was confirmed via library search and chemigrams were generated using the non-interfering IR spectral wavelengths of 966 cm⁻¹ for ammonia, 3744 cm⁻¹ for water, and 2359 cm⁻¹ for carbon dioxide. Samples for transmission electron microscopy (TEM) were prepared by drop-casting a suspension of **Ti_xM(ON)** in hexanes onto lacey-carbon-coated copper grids (Ted Pella, part no. 01824). Imaging was performed on a Philips CM-200 electron microscope operating at 200 kV. Compositional analysis was performed using an FEI Tecnai G2 F20 200 kV scanning transmission electron microscope (STEM) equipped with an Oxford energy dispersive X-ray spectrometer (EDS and EDS mapping). XPS analysis was performed on a Kratos Nova X-ray photoelectron spectrometer equipped with a monochromatic Al K α source operating at 300 W. Survey and high-resolution C 1s, O 1s, Mo 3d, Ti 2p and Mo 3p/N 1s spectra were acquired at 160 eV and 20 eV, while providing charge compensation using low energy electrons. Analysis and quantification of spectra were performed using CasaXPS software employing sensitivity factors supplied by the manufacturer. A linear background was applied to C 1s and O 1s, and a Shirley background was applied to Mo 3d, Ti 2p and Mo 3p/N 1s regions. Analysis included

charge referencing to the adventitious carbon signal at 285 eV. The time-resolved microwave conductivity (TRMC) technique is described thoroughly elsewhere.^{3,4} Briefly, the sample is deposited (drop-cast from mesitylene) on a quartz slide, which is mounted at the electric field maximum of a microwave resonance cavity tuned to 9 GHz. The photoconductivity of the sample is measured by monitoring the microwave power loss in the cavity as a function of time after exciting the sample with a 4 ns laser pulse. Excitation wavelengths were 355, 450 and 550 nm. Excitation fluence in all cases was ca. 10^{15} cm⁻².

MB decomposition. The decomposition of methylene blue (MB) dye was performed similarly to that previously described for UV-light driven decomposition using TiO₂.⁵ The initial concentration of MB was 3×10^{-5} M in ethanol, and the photocatalyst/MB ratio in the reaction was 1.0 g_{cat}/L. Prior to illumination, the photocatalyst/MB suspension was stirred in the dark for 10-15 min, and to account for the adsorption of MB on the catalyst, a 2 mL sample was taken, catalyst was removed by passing the solution through a 0.25 um syringe filter, and the absorption spectrum was recorded as t=0. The visible-light illumination source was a sulfur plasma lamp (LG Plasma System Model PSH0731WA) operating at ca. 100 mW/cm⁻² and using a 400 nm cutoff filter to eliminate UV-light. The reaction was continuously stirred, and at each interval, a 2 mL sample was taken, catalyst was removed using a syringe filter, and the absorption spectrum was recorded. The dye concentration at each illumination interval was determined using the dye absorption value at 655 nm. A control experiment following the visible-light degradation of the MB dye solution without any catalyst showed < 3% decrease in dye concentration after 3 h of illumination.

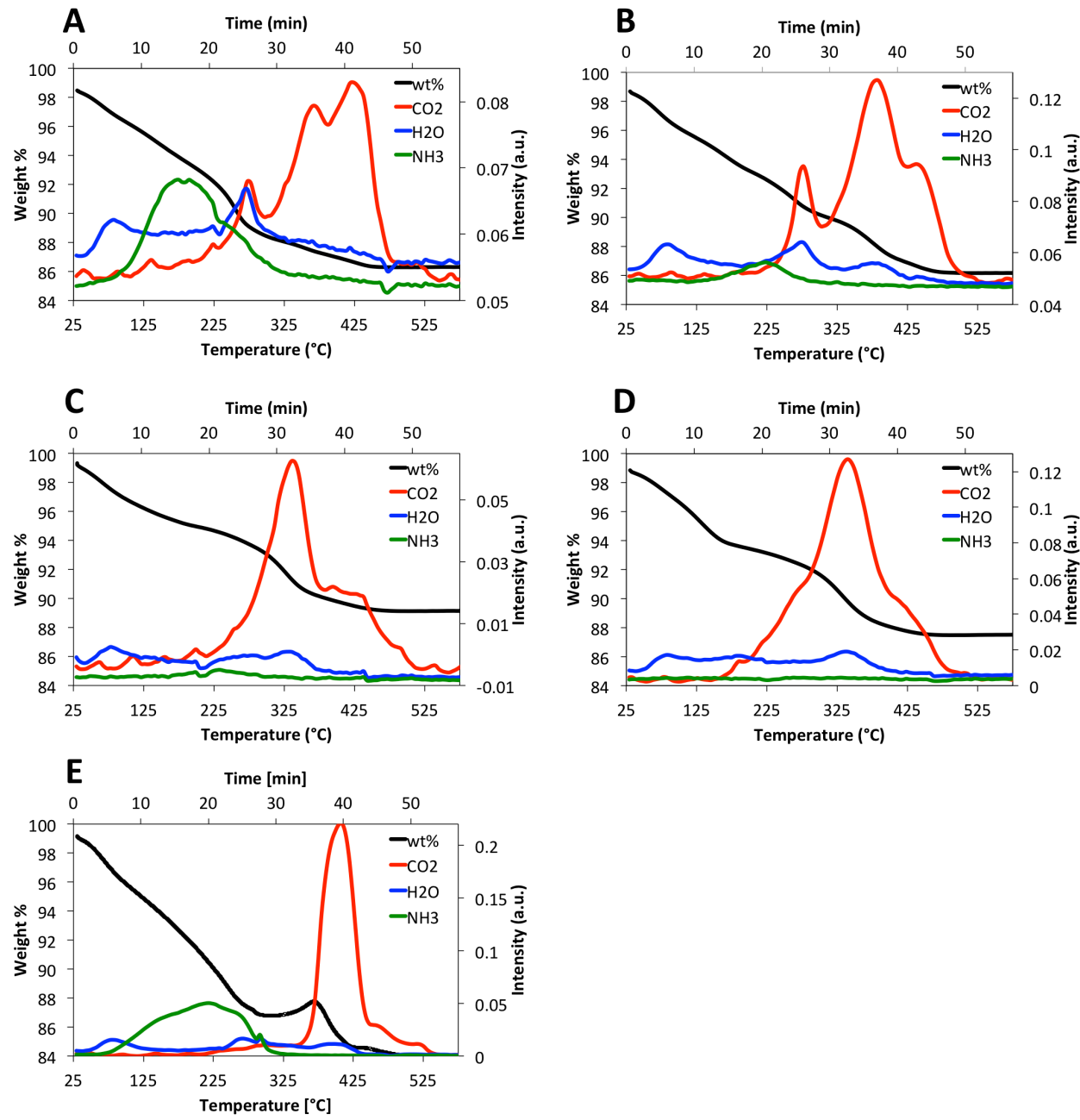


Fig. S1. TG-IR traces of (A) Ti₃M(ON), (B) Ti₁₀M(ON), (C) Ti₂₀M(ON), (D) Ti₁₀MoO, and (E) Mo(ON) materials under flowing air, heating rate 10 °C/min.

Table S1. Elemental analysis of Ti/Mo and N/Mo ratios and nitrogen porosimetry data for the $\text{Ti}_x\text{M}(\text{ON})$ and Ti_xMoO materials.

Material	Ti/Mo (mol/mol)	N/Mo (mol/mol)	%C (wt%)	S_{BET} (m^2/g)	V_p (cc/g)
Mo(ON)	—	0.78	3.65	9.61	0.026
Ti₃Mo(ON)	3.05	0.77	3.57	317	1.27
Ti₁₀Mo(ON)	10.2	0.75	3.50	386	1.97
Ti₂₀Mo(ON)	21.5	0.73	2.60	352	1.14
TiO ₂	—	—	—	200	0.687
Ti₃MoO	2.95	—	5.82	475	1.53
Ti₁₀MoO	10.0	—	4.43	325	0.916
Ti₂₀MoO	20.6	—	3.61	320	0.995

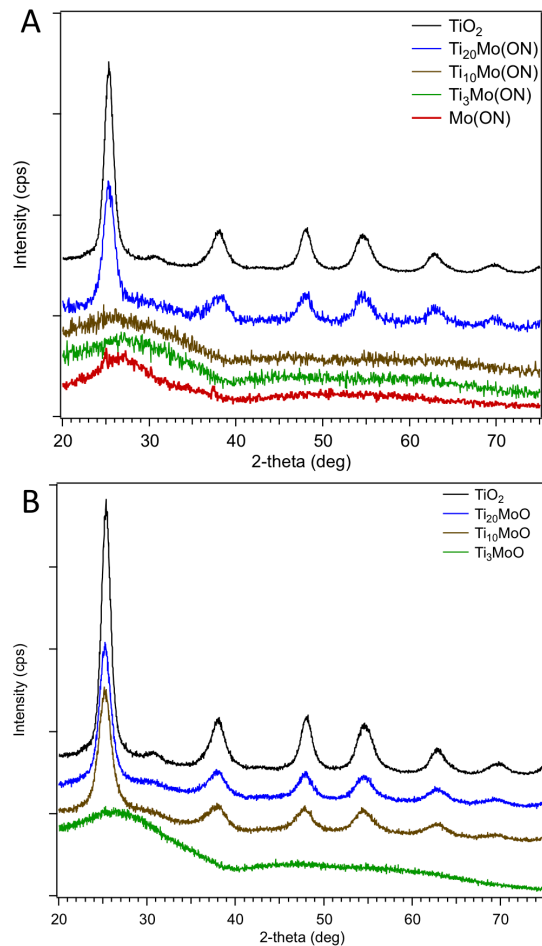


Fig. S2. PXRD patterns for (A) TiO₂, **Mo(ON)**, and $\text{Ti}_x\text{Mo(ON)}$ and (B) Ti_xMoO materials prepared from **1**, **2**, and **3**. Anatase (JCPDS 01-075-2544) and brookite (JCPDS 01-076-1937) phases were determined based on their respective JCPDS files.

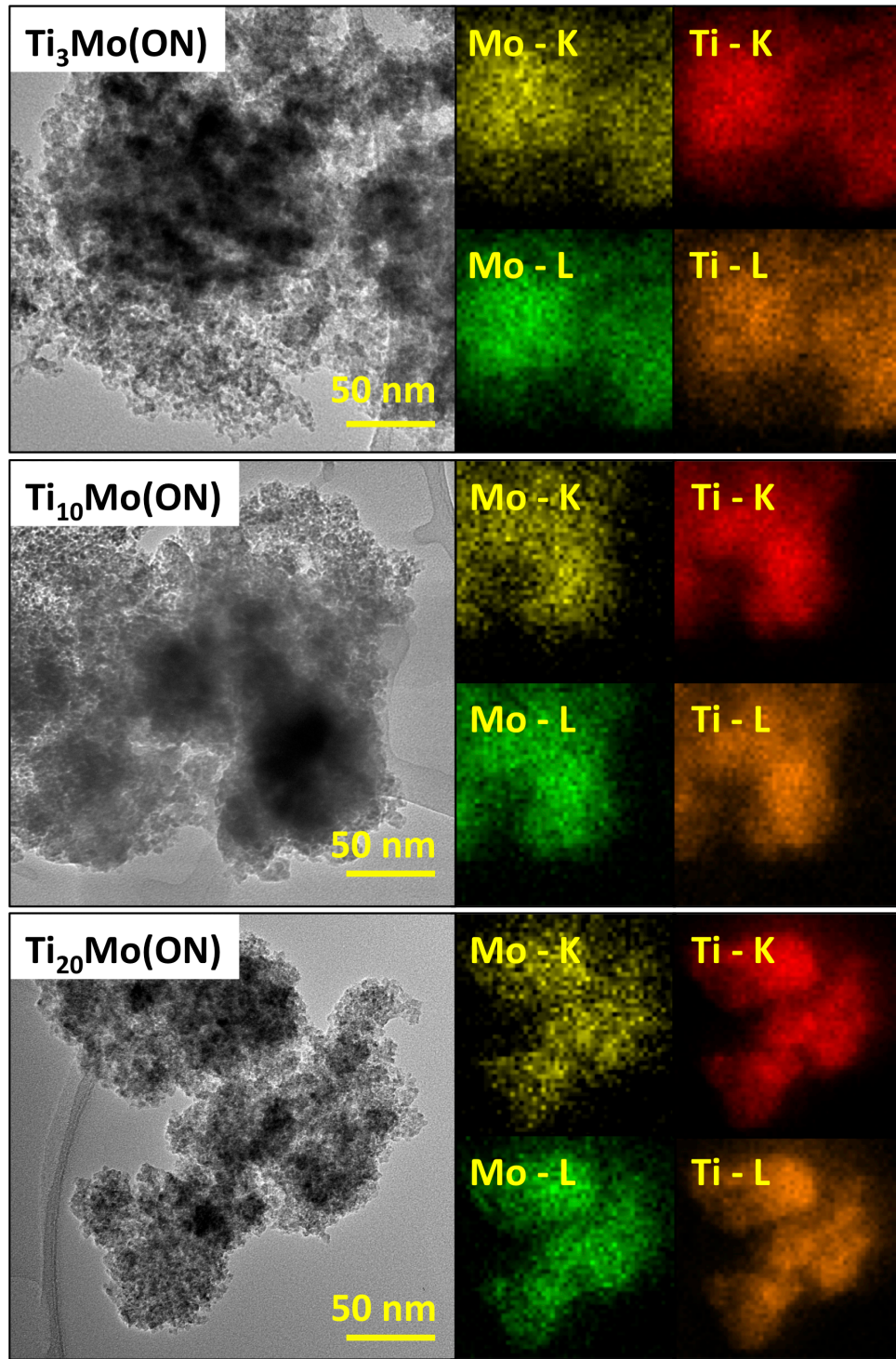


Fig. S3. Representative TEM images and EDS maps for $\text{Ti}_x\text{Mo(ON)}$ materials.

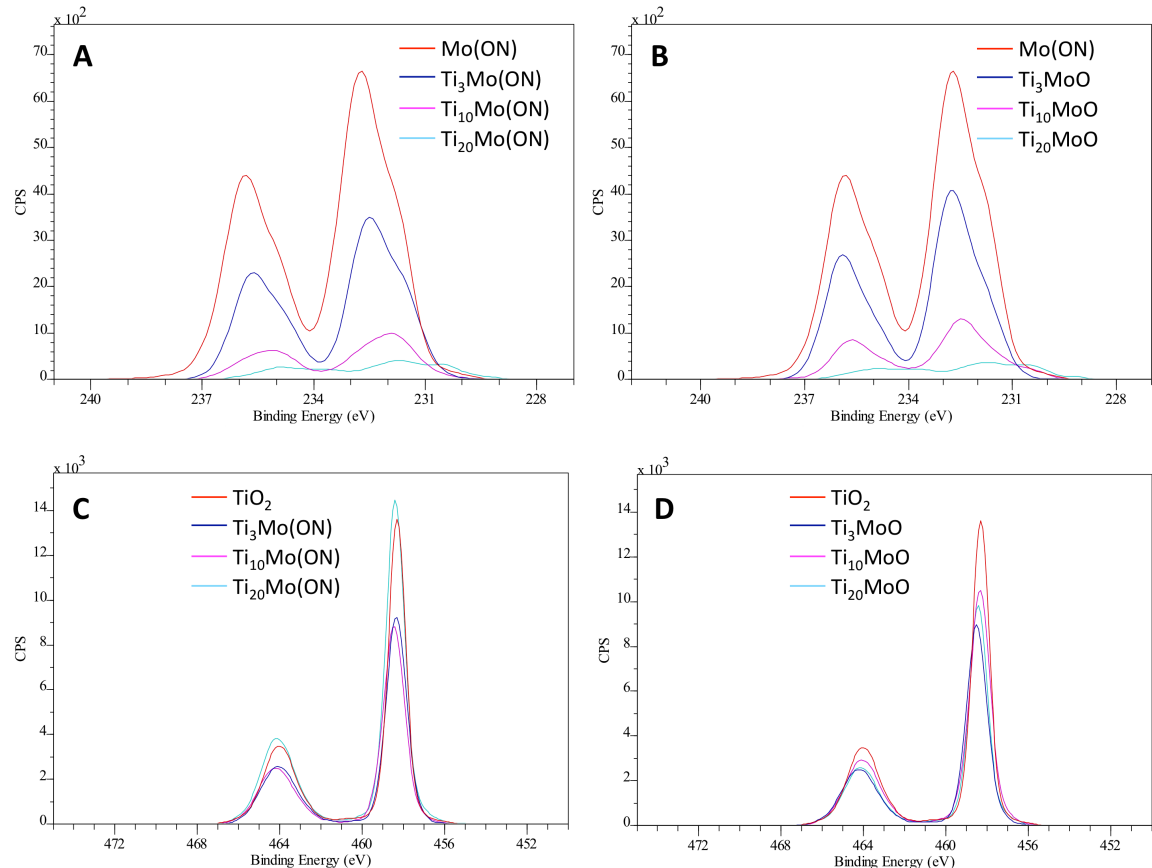


Fig. S4. Mo 3d XPS spectra for (A) Mo(ON) and $Ti_xMo(ON)$ materials and (B) Mo(ON) and Ti_xMoO materials. Ti 2p XPS spectra for (C) TiO_2 and $Ti_xMo(ON)$ materials and (D) TiO_2 and Ti_xMoO materials.

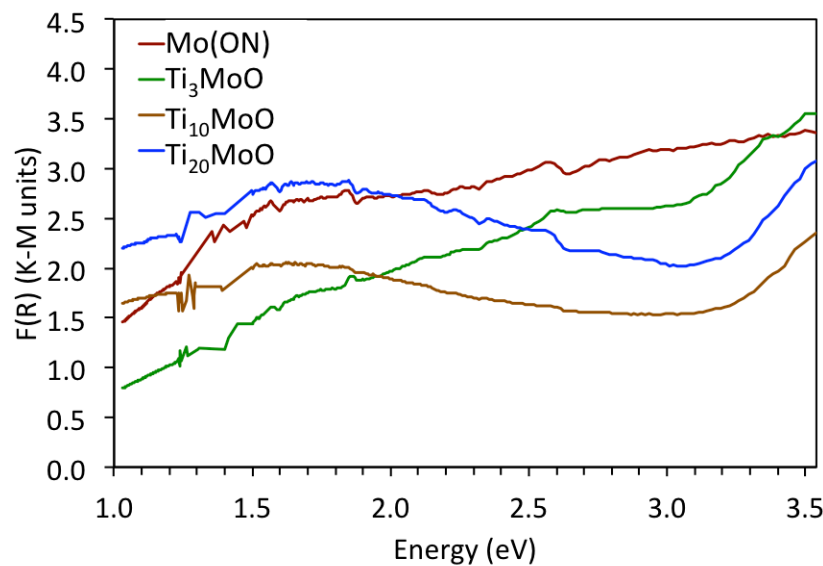
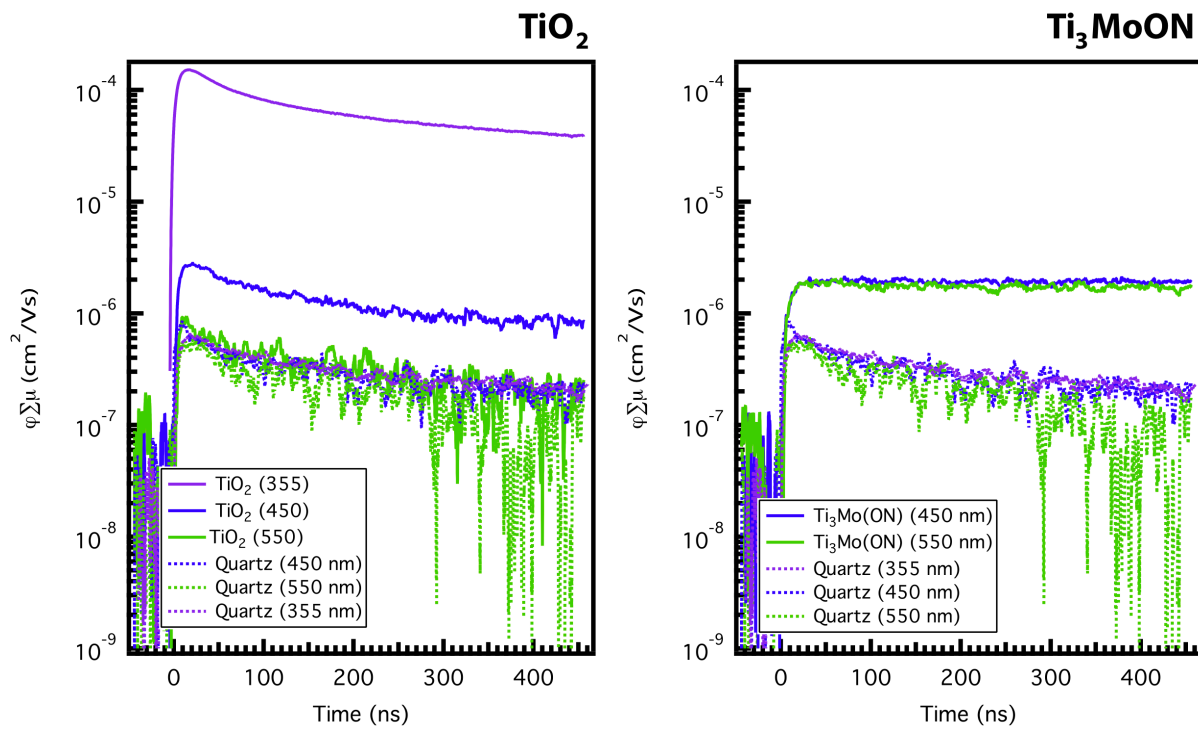


Fig. S5. DRUV-vis-NIR spectra for Mo(ON), Ti₃MoO, Ti₁₀MoO, and Ti₂₀MoO.



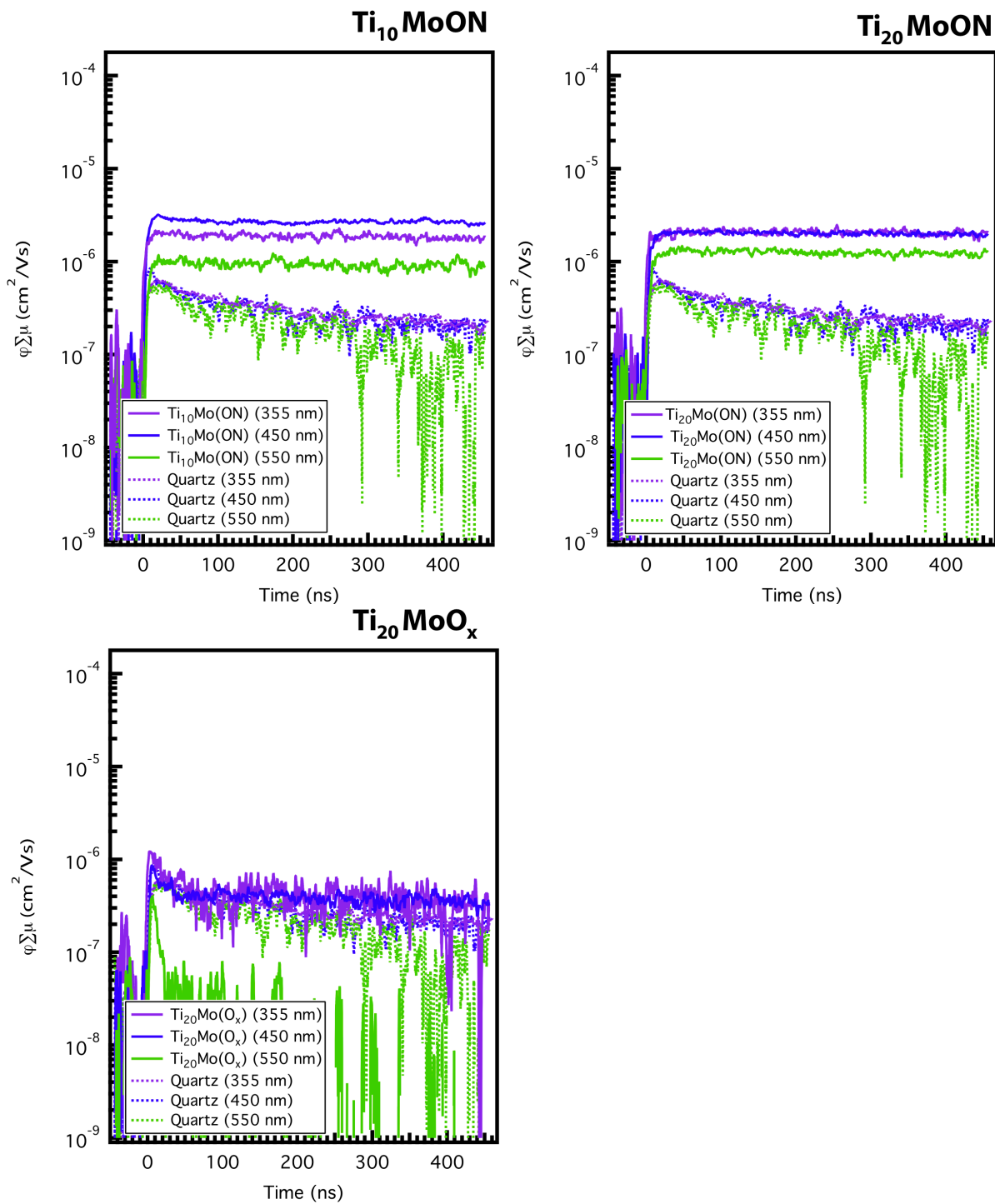


Fig. S6. Photoconductance transients of all samples measured, plotted as the product of charge carrier yield (ϕ) and the sum of the electron and hole mobilities ($\Sigma\mu$). Excitation fluence in all cases was $\sim 10^{15} \text{ cm}^{-2}$. Since the nitride-free material originated from the same procedures, equipment, and synthetic route as the oxynitride, yet shows no photoconductivity, these data additionally demonstrate that the photoconductivity observed in the oxynitride samples is not due to impurities.

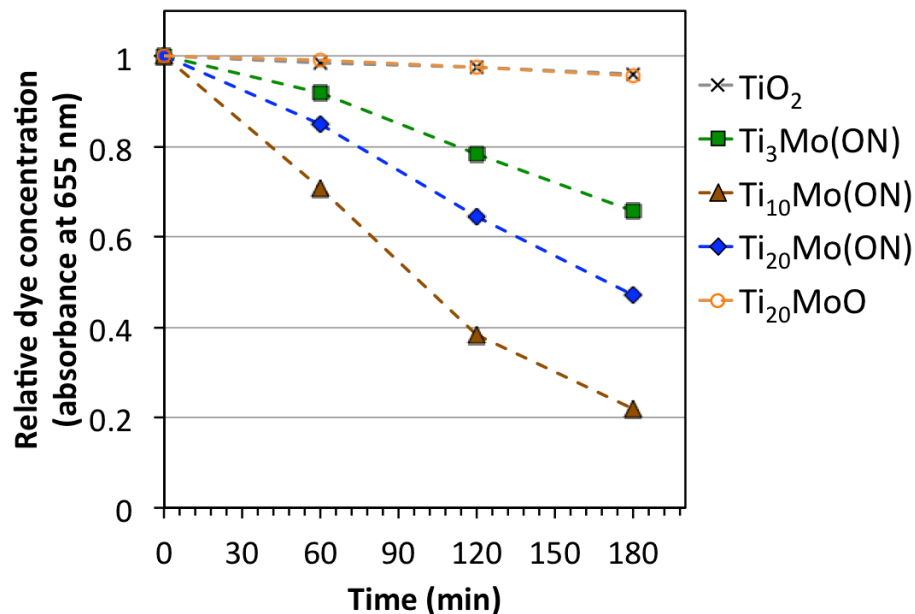


Fig. S7. Visible-light driven MB decomposition followed as a function of absorbance at 655 nm over TiO_2 (prepared from **2**), $\text{Ti}_x\text{Mo(ON)}$, and Ti_{20}MoO .

References

- 1 D. M. T. Chan, M. H. Chisholm, K. Folting, J. C. Huffman and N. S. Marchant, *Inorg. Chem.* 1986, **25**, 4170.
- 2 M. H. Chisholm, K. Folting, J. C. Huffman and C. C. Kirkpatrick, *Inorg. Chem.* 1984, **23**, 1021.
- 3 M. P. Dehaas and J. M. Warman *Chem. Phys.* 1982, **73**, 35.
- 4 J. E. Kroese, T. J. Savenije, M. J. W. Vermeulen and J. M. Warman, *J. Phys. Chem. B* 2003, **107**, 7696.
- 5 R. J. Tayade, T. S. Natarajan, H. C. Bajaj, *Ind. Eng. Chem. Res.* 2009, **48**, 10262.